Pairwise Data Consistency Conditions for the Exponential Fanbeam Transform

Richard Huber[1], Rolf Clackdoyle[1], and Laurent Desbat[1]

[1]Univ. Grenoble Alpes, CNRS, Grenoble INP, TIMC, 38000 Grenoble, France.

Abstract Data consistency conditions (DCCs) for projection operators have been of great relevance in the field of tomography, as they allow the determination of measured data's feasibility prior to reconstruction. Particularly useful are DCCs comparing two projections, accordingly called pairwise DCCs (PDCCs). Such conditions compute certain linear functionals dependent on individual projections, whose values must coincide for consistency to hold. For many projection operators, such PDCCs are known, but for the exponential fanbeam transform – which is relevant for Single Photon Emission Tomography (SPECT) – they are not. We show mathematically that no condition of this type can exist for a pair of exponential fanbeam projections. Moreover, we present a novel class of pairwise data consistency conditions, requiring that the difference between certain linear functionals of two projections lie in a specified interval, instead of coinciding as they would in classical PDCCs. This new condition is substantiated by numerical experiments (simulation study) on some phantoms.

1 Introduction

Tomographic techniques have become a vital tool in medicine, allowing doctors to observe patients' interior features. A mathematical operator (projection operator) models the underlying physics of the measurement process. The data is usually structured in so-called projections, referring to the data obtained during a specific measurement step. The choice of projection operator depends on the measurement setup used. The capability to determine whether measured data is consistent with the model/projection operator has found broad applications, such as identification/correction of corrupted data, geometric calibration, parameter identification, and motion detection [1–6]. Particularly useful are conditions capable of finding inconsistencies from just two projections, because small collections of arbitrarily oriented projections can be tested using such conditions. We refer to them as pairwise data consistency conditions (PDCCs).

A typical example is parallel-beam Computed Tomography (CT), which is modeled by the Radon transform

$$[\mathscr{R}f](\psi,s) := \int_{\mathbb{R}} f(s\vartheta_\psi^\perp + t\vartheta_\psi)\,\mathrm{d}t \tag{1}$$

for $\psi \in [0,\pi[$, $s\in\mathbb{R}$ and $f\in\mathscr{C}_c^\infty(\mathbb{R}^2)$ (smooth function with compact support), where $\vartheta_\psi = (\cos\psi,\sin\psi)^T$ and $\vartheta_\psi^\perp = (-\sin\psi,\cos\psi)^T$ are the projection directions with the angle ψ. In this case, the PDCCs are well-known [7]. For $\psi_1,\psi_2\in[0,\pi[$ and all $f\in\mathscr{C}_c^\infty(\mathbb{R}^2)$, they take the form

$$\int_{\mathbb{R}}[\mathscr{R}f](\psi_1,s)\,\mathrm{d}s = \int_{\mathbb{R}}[\mathscr{R}f](\psi_2,s)\,\mathrm{d}s. \tag{2}$$

We denote by $\mathscr{R}^\Lambda$ the operator $\mathscr{R}$ only containing two projections $\Lambda=(\psi_1,\psi_2)$; we call it the pairwise Radon transform. For several other projection operators, PDCCs have been found, two examples being the fanbeam operator [8] and the parallel-beam exponential operator [9]. One noticeable projection operator whose PDCC is yet unknown, is the (pairwise) exponential fanbeam transform

$$[\mathscr{E}_\mu^\Lambda f](\lambda,\phi) := \int_{\mathbb{R}^+} f(\lambda + t\vartheta_\phi)e^{\mu t}\,\mathrm{d}t \tag{3}$$

for $\lambda\in\Lambda=(\lambda_1,\lambda_2)\in\mathbb{R}^2\times\mathbb{R}^2$ (the fan vertex positions), $\phi\in[-\pi,\pi[$ and $f\in\mathscr{C}_c^\infty(\Omega)$ with constant attenuation parameter $\mu\in\mathbb{R}$. Here, Ω is an open, connected set whose compact closure does not intersect with the line containing λ_1 and λ_2. This operator finds applications in pinhole SPECT imaging and corresponding PDCCs could find applications in the alignment of SPECT/CT data [10]. Here, a projection corresponds to all rays converging on λ from any direction. The exponential term models constant attenuation processes; more general attenuation can – under certain assumptions – be converted to this exponential model, making this a mild restriction for many applications. Figure 1 illustrates the associated geometry. In this work, we explore PDCCs for the exponential fanbeam operator. For the conventional fanbeam transform ($\mu=0$), the PDDC has the form

$$\int_{-\pi}^{\pi}\frac{[\mathscr{E}_0^\Lambda f](\lambda_1,\phi)}{\vartheta_\phi^\perp\cdot\Delta}\,\mathrm{d}\phi = \int_{-\pi}^{\pi}\frac{[\mathscr{E}_0^\Lambda f](\lambda_2,\phi)}{\vartheta_\phi^\perp\cdot\Delta}\,\mathrm{d}\phi \tag{4}$$

with $\Delta=\lambda_2-\lambda_1$ [8]. Mathematically, (4) states that the function $\Big(1/(\vartheta_\phi^\perp\cdot\Delta),-1/(\vartheta_\phi^\perp\cdot\Delta)\Big)$ is orthogonal to $\mathrm{Rg}(\mathscr{E}_0^\Lambda)$, which corresponds to the backprojections of $1/(\vartheta_\phi^\perp\cdot\Delta)$ for both projections being equal. Other mentioned PDCCs are of similar mathematical structure. Hence, one might aim to find a pair of functions $\mathrm{G}_{\lambda_1,\lambda_2},\mathrm{G}_{\lambda_2,\lambda_1}$ such that

$$\int_{-\pi}^{\pi}[\mathscr{E}_\mu^\Lambda f](\lambda_1,\phi)\,\mathrm{G}_{\lambda_1,\lambda_2}(\phi)\,\mathrm{d}\phi = \int_{-\pi}^{\pi}[\mathscr{E}_\mu^\Lambda f](\lambda_2,\phi)\,\mathrm{G}_{\lambda_2,\lambda_1}(\phi)\,\mathrm{d}\phi \tag{5}$$

for all $f\in\mathscr{C}_c^\infty(\Omega)$. As we will show, there are no PDDCs of this form for the exponential fanbeam transform, i.e., (5) does not possess a solution.

2 Nonexistence of PDCCs

We first set some relevant notation. Since the map $(\phi,t)\mapsto\lambda+t\vartheta_\phi$ present in (3) is a diffeomorphism for any $\lambda\in\mathbb{R}^2$,

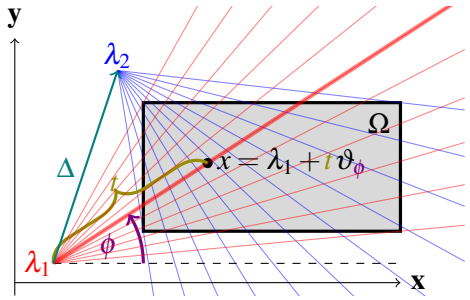

Figure 1: Illustration of the geometry of the fanbeam transform with two projections. The black point x on the bold red line and its parametrization in fanbeam coordinates with respect to the projection λ_1 is highlighted.

we define the inverse parametrizations

$$\phi_i(x) = \arg(x - \lambda_i) \qquad \text{and} \qquad t_i(x) = |x - \lambda_i| \tag{6}$$

for $i \in \{1,2\}$. Further, we define $\Omega' = (\{\lambda_1\} \times \Phi_1) \cup (\{\lambda_2\} \times \Phi_2)$ with $\Phi_i = \phi_i(\Omega)$ for $i \in \{1,2\}$; so Ω' is essentially a 2-projection sinogram domain.

Theorem 1. *There is no pair of non-zero functions* $\mathrm{G}_{\lambda_1,\lambda_2} \in L^1_{loc}(\Phi_1)$ *(functions absolutely integrable on any compact subset) and* $\mathrm{G}_{\lambda_2,\lambda_1} \in L^1_{loc}(\Phi_2)$ *such that* (5) *is satisfied for all* $f \in \mathscr{C}^\infty_c(\Omega)$ *when* $\mu \neq 0$.

Sketch of proof. We assume $\mathrm{G}_{\lambda_1,\lambda_2}$ and $\mathrm{G}_{\lambda_2,\lambda_1}$ non-zero satisfying (5) were to exist. Plugging the definition of the exponential fanbeam transform into (5) implies

$$\int_{\Phi_1}\int_{\mathbb{R}^+} f(\lambda_1 + t\vartheta_\phi) e^{\mu t}\,\mathrm{d}t\,\mathrm{G}_{\lambda_1,\lambda_2}(\phi)\,\mathrm{d}\phi = \int_{\Phi_2}\int_{\mathbb{R}^+} f(\lambda_2 + t\vartheta_\phi) e^{\mu t}\,\mathrm{d}t\,\mathrm{G}_{\lambda_2,\lambda_1}(\phi)\,\mathrm{d}\phi. \tag{7}$$

Substituting $x = \lambda_i + t\vartheta_\phi$ for $i \in \{1,2\}$, this is equivalent to

$$\int_\Omega f(x)\frac{\mathrm{G}_{\lambda_1,\lambda_2}(\phi_1(x))}{t_1(x)} e^{\mu t_1(x)}\,\mathrm{d}x = \int_\Omega f(x)\frac{\mathrm{G}_{\lambda_2,\lambda_1}(\phi_2(x))}{t_2(x)} e^{\mu t_2(x)}\,\mathrm{d}x. \tag{8}$$

Since this statement is assumed to be true for all $f \in \mathscr{C}^\infty_c(\Omega)$, the fundamental lemma of variational calculus implies

$$\frac{\mathrm{G}_{\lambda_1,\lambda_2}(\phi_1(x))}{t_1(x)} e^{\mu t_1(x)} = \frac{\mathrm{G}_{\lambda_2,\lambda_1}(\phi_2(x))}{t_2(x)} e^{\mu t_2(x)} \tag{9}$$

for almost all $x \in \Omega$. We show that this equation does not possess a solution (thus contradicting our original assumption) by setting

$$\mathrm{h}_{\lambda_1,\lambda_2}(\phi) = \mathrm{h}_{\lambda_2,\lambda_1}(\phi) = \frac{1}{\Delta \cdot \vartheta^\perp_\phi} \neq 0, \tag{10}$$

which, for all $x \in \Omega$, satisfies

$$\frac{\mathrm{h}_{\lambda_1,\lambda_2}(\phi_1(x))}{t_1(x)} = \frac{\mathrm{h}_{\lambda_2,\lambda_1}(\phi_2(x))}{t_2(x)}. \tag{11}$$

Hence, we set $\mathrm{g}_{\lambda_1,\lambda_2} := \ln(\mathrm{G}_{\lambda_1,\lambda_2} / \mathrm{h}_{\lambda_1,\lambda_2})$ and $\mathrm{g}_{\lambda_2,\lambda_1} := \ln(\mathrm{G}_{\lambda_2,\lambda_1} / \mathrm{h}_{\lambda_2,\lambda_1})$ which (combining (9), (11)) satisfies

$$\mathrm{g}_{\lambda_1,\lambda_2}(\phi_1(x))) - \mathrm{g}_{\lambda_2,\lambda_1}(\phi_2(x)) = \mu(t_2(x) - t_1(x)). \tag{12}$$

Moreover, expressing $t_1(x) - t_2(x)$ explicitly via basic computation – e.g., using the Law of Sines – shows that

$$\mathrm{g}_{\lambda_1,\lambda_2}(\phi_1) - \mathrm{g}_{\lambda_2,\lambda_1}(\phi_2) = \mu\frac{\Delta \cdot (\vartheta^\perp_{\phi_1} - \vartheta^\perp_{\phi_2})}{\vartheta^\perp_{\phi_1} \cdot \vartheta_{\phi_2}} \tag{13}$$

for all $\phi_1 \in \Phi_1$ and $\phi_2 \in \Phi_2$. It seems dubious that the right-hand side of (13) can be the sum of functions only depending on ϕ_1 or ϕ_2, respectively, as required by the left-hand side. Proving that is slightly technical, so we do not go into detail here, but roughly speaking it involves observing that the left-hand side of

$$\mathrm{g}_{\lambda_1,\lambda_2}(\phi_1) - \mathrm{g}_{\lambda_1,\lambda_2}(\widetilde{\phi}_1) = \mu\frac{\Delta \cdot (\vartheta^\perp_{\phi_1} - \vartheta^\perp_{\phi_2})}{\vartheta^\perp_{\phi_1} \cdot \vartheta_{\phi_2}} - \mu\frac{\Delta \cdot (\vartheta^\perp_{\widetilde{\phi}_1} - \vartheta^\perp_{\phi_2})}{\vartheta^\perp_{\widetilde{\phi}_1} \cdot \vartheta_{\phi_2}} \tag{14}$$

does not depend on ϕ_2, but the right-hand side does, as can be verified via evaluation for certain values $\phi_1, \widetilde{\phi}_1, \phi_2$ when $\mu \neq 0$. Since the function in (14) is analytical when the denominator is not zero, the equation is wrong for almost every tuple, particularly the ones representing Ω. So (13) has no solution, and consequently neither does (9), as required to prove the theorem. □

Many of the steps in the proof of Theorem 1 are not specific to the exponential fanbeam transform, but also apply to other projection pair operators. Thus the approach can be used to check if a projection pair operator possesses a PDCC, and also gives a method for identifying them if they do.

Not only range conditions of the specific form (5) cannot exist, but in fact, no $L^2(\Omega')$-continuous conditions of any kind can; even if they were non-linear.

Theorem 2. *When* $\mu \neq 0$*, there is no continuous function* $F\colon L^2(\Omega') \to \mathbb{R}$ *which satisfies*

1. $F(g) = 0$ *when* $g \in \mathrm{Rg}(\mathscr{E}^\Lambda_\mu)$,
2. *There is* $g \in L^2(\Omega')$ *with* $F(g) \neq 0$.

Sketch of proof. As a direct consequence of Theorem 1, the range of $\mathscr{E}^\Lambda_\mu$ must be dense in $L^2(\Omega')$ as no non-trivial orthogonal vector exists. If F as described were to exist, it would be zero on a dense set, and by continuity zero everywhere, contradicting the second point. □

Real world data are always imperfect – and therefore inconsistent. A DCC which is continuous will be nearly satisfied for very mildly inconsistent data. Thus, a continuous DCC is favored in practice, even though it can only identify the closure of the range. It is not yet known, whether the range of the exponential fanbeam transform is closed.

3 Alternative consistency conditions

That no PDCCs exist, does not imply that there is no overlapping information whatsoever. There might still be a large class of functions for which some kind of consistency criteria are possible.

Evidently, the ratio for λ_1 to λ_2 of the exponential weight applied by $\mathscr{E}_\mu^\Lambda$ to any point x is $e^{\mu(t_1(x)-t_2(x))}$, and aside from this factor, the measurements behave like conventional fanbeam data ($\mu = 0$). Hence, we define

$$\overline{\delta}_\mu = \max_{x\in\Omega}\Big(\mu\big(t_1(x)-t_2(x)\big)\Big), \quad \underline{\delta}_\mu = \min_{x\in\Omega}\Big(\mu\big(t_1(x)-t_2(x)\big)\Big).$$

Theorem 3. *Let $f \in \mathscr{C}_c^\infty(\Omega)$ with $f \geq 0$ not constantly zero. Then*

$$\left(\frac{\int_{-\pi}^{\pi}[\mathscr{E}_\mu^\Lambda f](\lambda_1,\phi)\frac{1}{\vartheta_\phi^\perp\cdot\Delta}\,\mathrm{d}\phi}{\int_{-\pi}^{\pi}[\mathscr{E}_\mu^\Lambda f](\lambda_2,\phi)\frac{1}{\vartheta_\phi^\perp\cdot\Delta}\,\mathrm{d}\phi}\right) \in \left[e^{\underline{\delta}_\mu}, e^{\overline{\delta}_\mu}\right]. \qquad (15)$$

Note that the left-hand side of (15) (henceforth called consistency quotient) would be 1 for the conventional fanbeam transform (see (4)). So this condition states that the exponential fanbeam transform satisfies the conventional fanbeam transform's PDCC within a certain margin dependent on the geometry (the extent of Ω and positions λ_1, λ_2) and the attenuation coefficient.

Satisfying (15) does not guarantee consistency, as mildly inconsistent data might still be within the bounds. However, violating the condition implies inconsistency with certainty.

This result does not contradict Theorem 2 since the consistency quotient in (15) is not continuous at $f = 0$. For f giving a non-zero denominator in (15), the denominator does not become zero when sufficiently small noise is added, making the condition stable under low noise conditions.

Sketch of proof. We define the function $\widetilde{f}(x) = f(x)e^{\mu(t_1(x)-t_2(x))}$ and the conventional fanbeam's PDCC (4) for $f(x)e^{\mu t_1(x)}$ implies

$$\int_{-\pi}^{\pi}[\mathscr{E}_\mu^\Lambda f](\lambda_1,\phi)\frac{1}{\vartheta_\phi^\perp\cdot\Delta}\,\mathrm{d}\phi = \int_{-\pi}^{\pi}[\mathscr{E}_\mu^\Lambda \widetilde{f}](\lambda_2,\phi)\frac{1}{\vartheta_\phi^\perp\cdot\Delta}\,\mathrm{d}\phi. \qquad (16)$$

Moreover, using the mean value theorem, it is easy to see that

$$\frac{[\mathscr{E}_\mu^\Lambda \widetilde{f}](\lambda_2,\phi)}{[\mathscr{E}_\mu^\Lambda f](\lambda_2,\phi)} \in \left[e^{\underline{\delta}_\mu}, e^{\overline{\delta}_\mu}\right]. \qquad (17)$$

Combining the right-hand side of (16) with (17) and basic integration properties, Theorem 3 follows directly. □

4 Numerical experiments

We conducted numerical experiments to corroborate Theorem 3's result and to show that the interval proposed in (15) is not chosen needlessly big, but is violated by inconsistent enough data. To that end, we considered the following setup: We had fan vertex positions $\lambda = 80\vartheta_\varphi$ for $\varphi = \{-90°, -88°, \ldots, 88°, 90°\}$. The imaging domain was a 40 cm × 40 cm square centered at the origin, and the attenuation parameter $\mu = -0.154$ (the attenuation per cm of water). We chose $\Omega = [-20\,\mathrm{cm}, 20\,\mathrm{cm}] \times [-14\,\mathrm{cm}, 8\,\mathrm{cm}]$ reflecting a box with width and height to encompass the activity. We computed the consistency quotient for two activity distributions designed to highlight specific aspects of Theorem 3. Those activities were the NCAT phantom [11] and a (Hot Source) phantom with constant activity in a circle with radius 1 cm at the bottom right extremity of Ω. Those phantoms were digitally represented on an array of $N_x \times N_x$ pixels with $N_x = 400$ and were transformed into sinograms with $N_s = 200$ detector pixels positioned equispaced on a flat detector covering the relative angular range of $[-\arctan\left(\frac{5}{12}\right), \arctan\left(\frac{5}{12}\right)]$; see Figure 2. The exponential fanbeam transform was executed with Gratopy [12] employing a pixel-driven approach. We simulated motion inconsistencies by shifting the phantom for projections with $\varphi > 4°$ by 4 cm in the x-direction. This corresponded to an abrupt movement of the patient at 8 minutes after the beginning of a 15-minutes scan.

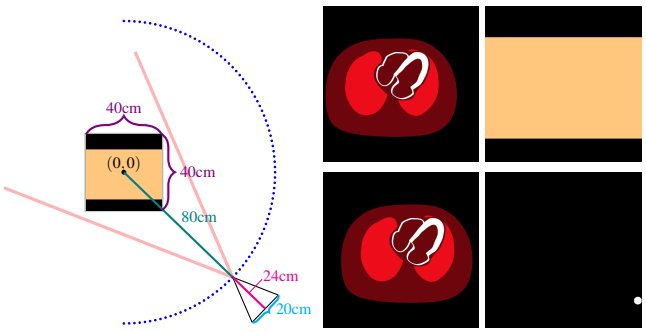

Figure 2: Illustration of the geometry used for numerical experiments, with the blue dots representing the fan vertex positions. The central 40 cm × 40 cm box represents the imaging domain containing activity overlayed with an illustration of our choice of Ω. On the right: (upper left) the NCAT phantom and its shifted form (lower left), (upper right) the rectangular domain Ω and (lower right) the second phantom consisting of a hot source located in the bottom right corner of Ω.

Figure 3 depicts the evaluation of condition (15) for the two scenarios by showing the consistency quotient for the middle projection (associated with $\varphi = 0$) paired with any other λ, and the corresponding bounds (the right-hand side of (15)). For the NCAT phantom without motion (consistent projections) the consistency quotient remained close to one, and stayed well within the bounds given by Theorem 3. For the NCAT phantom with motion, the consistency quotient behaved similarly, but did violate the consistency bounds for projections near the reference projection. For the second phantom, the data were consistent (no motion) and, as expected, the consistency quotient remained within the bounds, but closely followed the upper right arm of the bounds, which supports the notion that these bounds cannot be improved

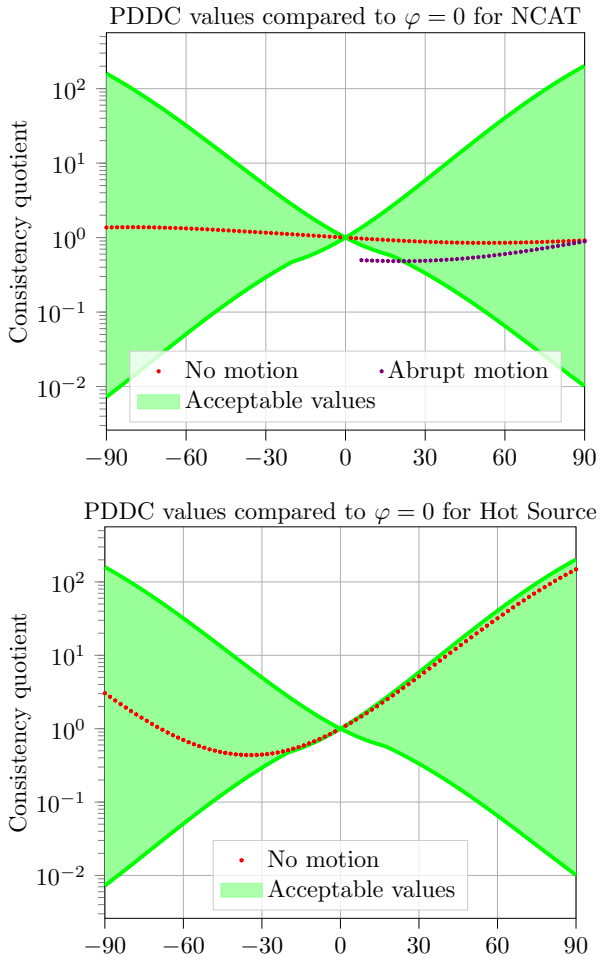

Figure 3: Evaluation of (15) in the numerical experiments, on the top for the NCAT phantom, below the second phantom. The consistency quotient of the consistent measurements and the inconsistent measurments with motion at the 8-minute mark are depicted. These observations are made for $\lambda_1 = \vartheta_\varphi$ with the angle $\varphi = 0$, while the angles of λ_2 are on the **x**-axis.

when using this particular consistency quotient. Simulations with the hot source in the other three corners of the rectangular support region result in tracing the other three arms of the bounds.

5 Summary and Outlook

This paper discussed data consistency conditions for the exponential fanbeam transform, showing that (classical) pairwise data consistency conditions cannot exist for this transform. As an alternative, Theorem 3 provides a weak form of PDCC whereby a certain expression, the consistency quotient, must lie within a defined interval if the two projections are consistent. The NCAT simulations illustrated three consequences of Theorem 3, namely (i) that if the projections are consistent, the consistency quotient will lie within the bounds defined by the interval; (ii) equivalently, values lying outside the bounds definitely indicate inconsistency; and (iii) values inside the bounds do not provide information on consistency. For similar projections (fanbeam vertex positions fairly close to each other) the bounds are reasonably small and effectively detected inconsistency. For distant projections though, the bounds can be very broad, which limits their usefulness. However, the functional in (15) can probably be improved upon, to achieve tighter bounds and a consequently stronger PDCC. This might be the topic of future work.

We have illustrated the potential for patient motion identification, but other applications, such as detector sensitivity response or identification of pinhole positions, are conceivable.

Acknowledgement: This work was supported by the ANR grant ANR-21-CE45-0026 ‘SPECT-Motion-eDCC’.

References

[1] F. Natterer. “Computerized Tomography with Unknown Sources”. *SIAM Journal on Applied Mathematics* 43.5 (1983), pp. 1201–1212. DOI: 10.1137/0143079.

[2] A. Welch, R. Clack, F. Natterer, et al. “Toward accurate attenuation correction in SPECT without transmission measurements”. *IEEE transactions on medical imaging* 16 (1997), pp. 532–41. DOI: 10.1109/42.640743.

[3] A. Alessio, J. Caldwell, G. Chen, et al. “Attenuation-Emission Alignment in Cardiac PET/CT with Consistency Conditions”. *IEEE Nuclear Science Symposium Conference Record*. 2006, pp. 3288 –3291. DOI: 10.1109/NSSMIC.2006.353710.

[4] J. Xu, K. Taguchi, and B. Tsui. “Statistical Projection Completion in X-ray CT Using Consistency Conditions”. *IEEE Trans. Med. Imaging* 29 (2010), pp. 1528–1540. DOI: 10.1109/TMI.2010.2048335.

[5] R. Clackdoyle and L. Desbat. “Data consistency conditions for truncated fanbeam and parallel projections.” *Medical physics* 42 2 (2015), pp. 831–45.

[6] J. Lesaint, S. Rit, R. Clackdoyle, et al. “Calibration for Circular Cone-Beam CT Based on Consistency Conditions”. *IEEE Transactions on Radiation and Plasma Medical Sciences* 1.6 (2017), pp. 517 –526. DOI: 10.1109/TRPMS.2017.2734844.

[7] F. Natterer. *The Mathematics of Computerized Tomography*. Philadelphia: Society for Industrial and Applied Mathematics, 2001. Chap. II.4.

[8] D. V. Finch and D. C. Solmon. “Sums of homogeneous functions and the range of the divergent beam x-ray transform”. *Numerical Functional Analysis and Optimization* 5.4 (1983), pp. 363–419. DOI: 10.1080/01630568308816147.

[9] V Aguilar and P Kuchment. “Range conditions for the multidimensional exponential X-ray transform”. *Inverse Problems* 11.5 (1995), p. 977. DOI: 10.1088/0266-5611/11/5/002.

[10] G. Wells and R. Clackdoyle. “Feasibility of attenuation map alignment in pinhole cardiac SPECT using exponential data consistency conditions”. *Medical Physics* 48(9) (2021), pp. 4955–4965. DOI: 10.1002/mp.15058.

[11] W. Segars and B. Tsui. “Study of the efficacy of respiratory gating in myocardial SPECT using the new 4D NCAT phantom”. *2001 IEEE Nuclear Science Symposium Conference Record*. Vol. 3. 2001, pp. 1536–1539. DOI: 10.1109/NSSMIC.2001.1008630.

[12] K. Bredies and R. Huber. *Gratopy 0.1 release candidate 1 [software]*. Zenodo, 2021, https://doi.org/10.5281/zenodo.5221443. Version v0.1.0-beta.0. 2021. DOI: 10.5281/zenodo.5221443.